Nanomedicine Journal

Original Research

Preparation and characterization of hydroxyapatite reinforced with hardystonite as a novel bio-nanocomposite for tissue engineering

Hassan Gheisari[1*], Ebrahim Karamian[2]

[1]Department of Materials Engineering, Shahreza Branch, Islamic Azad University, Shahreza, Isfahan, Iran
[2]Advanced Materials Research Center, Department of Materials Engineering, Najafabad Branch, Islamic Azad University, Najafabad, Isfahan, Iran

Abstract

Objecttive(s): Despite the poor mechanical properties of hydroxyapatite, its unique biological properties leads we think about study on improving its properties rather than completely replacing it with other biomaterials. Accordingly, in this study we introduced hydroxyapatite reinforced with hardystonite as a novel bio-nanocomposite and evaluate its in-vitro bioactivity with the aim of developing a mechanically strong and highly porous scaffold for bone tissue engineering applications.

Materials and Methods: Natural Hydroxyapatite (NHA)-Hardystonite (HT) nanocomposite with different percentage of HT was synthesized by mechanical activation method and subsequent heating annealing process. This study showed that the addition of HT to HA not only increases the mechanical properties of HA but also improves its bioactivity. Dissolution curves presented in this study indicated that the pH value of SBF solution in the vicinity of HA-HT nanocomposite increases during the first week of experiment and decreases to blood pH at the second weekend. Hardystonite was composed of nano-crystalline structure with approximately diameter 40 nm. Specimens were composed of a blend of pure calcite ($CaCO_3$) (98% purity, Merck), silica amorphous (SiO_2) (98% purity, Merck) powder and pure zinc oxide (ZnO) with 50 % wt., 30 %wt and 20 %wt., respectively. These powders were milled by high energy ball mill using ball-to- powder ratio 10:1 and rotation speed of 600 rpm for 5 and 10 h. Then, the mixture mechanical activated has been pressed under 20 MPa. The samples pressed have been heated at 1100 ºC for 3 h in muffle furnace at air atmosphere. X-ray diffraction (XRD), scanning electron microscopy (SEM) and BET performed on the samples to characterize.

Results: According to XRD results, the sample milled for 10 h just indicated the hardystonite phase, while the sample milled for 5 h illustrate hardystonite phase along with several phases.

Conclusion: In fact, our study indicated that hardystonite powder was composed of nano-crystalline structure, about 40 nm, can be prepared by mechanical activation to use as a new biomaterials for orthopedic applications.

Keywords: Ball milling, Hardystonite, Hydroxyapatite, Nano composite

*Corresponding author: Hassan Gheisari, Department of Materials Engineering, Shahreza Branch, Islamic University of Shahreza, Iran.
Tel: +989135344540, Email: Hassan.gh.d@gmail.com

Introduction

Although, hydroxyapatite (HA) is the most investigated ceramic material for creating bone tissue scaffolds as it is the major inorganic component of natural bone and biocompatible. But, its mechanical strength is inadequate and it is too brittle and fracture frequently – making it suitable only for low load-bearing applications [1, 2]. Calsim and silicon ions, both of which are essential elements for human body, have been proved to promote osteoblast proliferation and differentiation. They have been utilized to chemically modify biomaterials for enhanced bioactivity. Calcium silicates including $CaSiO_3$ and Ca_2SiO_4 are the most typical ceramic materials capable of releasing Ca and Si ions and their potential for use in bone replacement and regeneration applications have been demonstrated in vitro and in vivo. As in recent years, calcium silicate-based ceramics have shown promise as bone implant materials, opening new avenues in the biomaterials field [3, 4].

However, a major drawback of the $CaSiO_3$ceramics is their high dissolution rate, which leads to an increased pH value in the environment that is lethal for cells [3]. In addition, the CS cannot support human bone cell proliferation [5] .These drawbacks were addressed by incorporating ZnO into $CaSiO_3$ [6, 7]. Zinc is an essential trace element that also plays an important role in bone metabolism. The stimulatory action of Zn on bone protein, bone formation and alkaline phosphatase activity was studied by Yagamuchi et al. in both in vitro and in vivo conditions. Therefore, Zn containing ceramic composites provide new possibilities in bone tissue engineering research. Ito et al. reported that Zn substituted tricalcium phosphate (Zn-TCP) apatite enhanced cell proliferation. Zinc added aluminate ceramic also had stimulatory action on osteoblast cells and favored the differentiation and mineralization process [1].

Wu et al. incorporated Zn into calcium silicate and synthesized hardystonite ($Ca_2ZnSi_2O_7$) which had better mechanical strength than HA [1]. Hardystonite is more chemically stable compared to CS ceramics and the presence of Zn ions affects the roughness of the ceramic [8]. Moreover, $Ca_2ZnSi_2O_7$ceramics supported human osteoblast-like cells (HOB) attachment, proliferation and differentiation and increased the alkaline phosphatase activity as reported by Ramaswamy et al. [3].

Currently, two common methods have been used for testing the in vitro bioactivity of bioceramics. One method is to evaluate the apatite-formation ability of bioceramics in the simulated body fluids (SBF). The other method is to investigate in vitro bone cell response to bioceramics. The SBF method is a useful way to test the in vitro bioactivity of bioceramics for the assessment of the apatite formation potential. However, the reliability this method depends on the category of bioceramics tested. Silicate-based bio-ceramics, have been shown to have excellent apatite forming abilities in SBF [9]. Bioactivity is defined as the property of the material to develop a direct, adherent, and strong bonding with the bone tissue. To evaluate this bioactivity of the materials, it has been proposed that materials that form an appetite on their surfaces in the SBF also can form the apatite in a living body and can bond to bone through the apatite layer. In other words, the apatite-forming ability in the SBF is a measure of in vivo bioactivity [10]. Despite the poor mechanical properties of hydroxyapatite, its unique biological properties leads we think about study on improving its properties rather than completely replacing it with other biomaterials. Accordingly, in this study we introduced a new HA-HT composite biomaterial and evaluate its in-vitro bioactivity with the aim of developing a mechanically strong and highly porous

scaffold for bone tissue engineering applications.

Materials and method
Material preparation
In this study, a clean veal bone was cut into small pieces and treated with sodium hydroxide solution in a beaker to remove organics until the color of bone turn into white.After neutralized with distilled water the bones were dried in oven and heat treated at 800 °C for 3 hours to completely remove organics part. Proteins free HA bone were then ground into fine powder by using planetary ball milling for several hour. The XRF analysis of produced hydroxyapatite powders is shown in Table 1. The most characteristic chemical groups in the FTIR spectrum of synthesized NHA are $PO4^{3-}$, OH^-, CO_3^{2-}, as well as HPO_4^{2-} that characterize nonstoichiometric HA

(Figure 1). PO_4^{3-} group forms intensive IR absorption bands at 560 and 600 cm^{-1} and at 1000–1100 cm^{-1}. Adsorbed water band is relatively wide, from 3600 to 2600 cm^{-1}, with an explicit peak at 3570 cm^{-1}; a weaker peak is formed at 630 cm^{-1}. C-O intensive peaks between 1460 and 1530 cm^{-1} which represent natural HA. The HT powders were synthesized by the high energy ball milling method using $CaCO_3$ (99%, Merck), ZnO (99%, Merck) and SiO_2 (99%- Merck) powders. Briefly, stoichiometric amounts of the mentioned raw materials milled under a ball to powder weight ratio of 10 and a vial velocity of 600 rpm, for 10 hours. The process continued with the uniaxial pressing of the Hardystonite powders at 10 MPa followed by sintering at 1200 °K for 3 hours and milling for 1 hour to produce HT powders with high reactivity.

Table 1. The XRF analysis of produced hydroxyapatite powders.

Element	Ca	P	Na	F	Mg	Sr	Cl	Si	S	Al	Cu	Zn	Fe	K	Zr	Ca/P	Total
Wt%	70.2	21.09	1.14	1.09	0.64	0.40	0.18	0.12	0.06	0.05	0.05	0.04	0.04	0.02	0.007	3.33	100.04
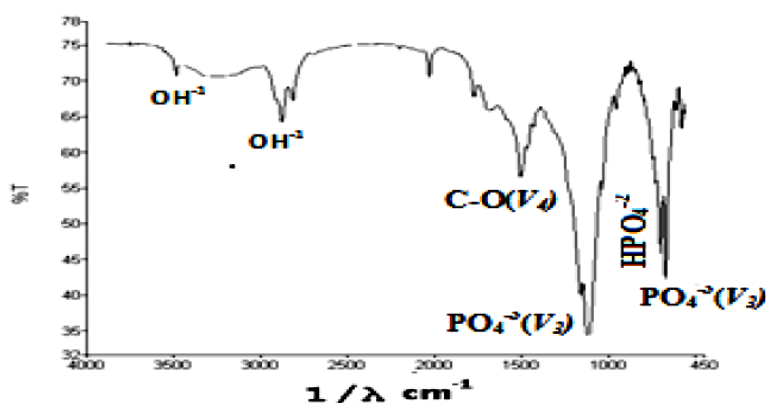
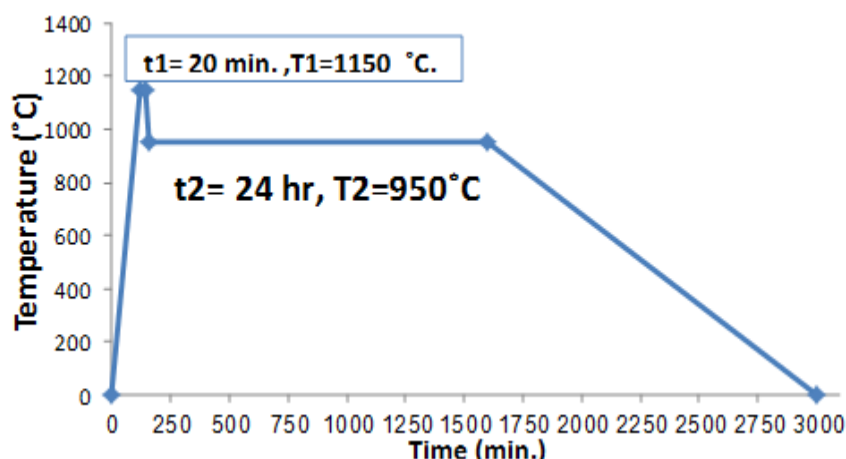**Figure 1.** FTIR spectrum of produced hydroxyapatite powder.

Figure 2. Two step sintering (TSS) process to compact the nanocomposite samples.

Composite building

An HA-HS nanocomposite powder with different percentages of HT (5 , 10 and 15 wt%) nanoparticles, was synthesized via high energy ball milling. BPR was 10; the speed of vial was 600 rpm. The nanocomposite powder then pressed under 60 MPa pressure and the produced samples sintered via two step sintering (TSS) process as shown in Figure 2.

Evaluation of bioactivity

In this study, simulated body fluid (SBF) was used to evaluate the bioactivity behavior. It is consist of their immersion in an aqueous SBF solution which simulates the properties of human plasma for certain period and verifies the formation of the hydroxyapatite (HA).

layer on the surface of the samples [11]. Simulated body fluid is prepared in laboratory with the ionic concentration nearly similar to human blood plasma [12]. The simulated body fluid is prepared according to procedure developed by Kokubo (Kokubo method) [13].

The appropriate quantities of reagents like NaCl, NaHCO$_3$, KCl, K$_2$HPO$_4$·3H$_2$O, MgCl$_2$·6H$_2$O, CaCl$_2$, Na$_2$SO$_4$, and tris buffer are dissolved in 1 l of double distilled water so as to have ionic concentration of various inorganic ions similar to those of the human blood plasma [12].

Table 2 gives the ion concentration of SBF prepared following Kokubo method and its comparison with human blood plasma.

Table 2. Ion concentrations (mmol/dm^3) of SBF and Human Blood Plasma.

Ionic concentration (mmol/dm^3)	Simulated body fluid	Blood plasma
Na$^+$	142	142
K$^+$	5	5
Mg^{+2}	1.5	1.5
Ca^{+2}	2.5	2.5
Cl$^-$	147.8	103
HCO^{-3}	4.2	27
HPO$_4^{-2}$	1	1
SO$_4^{-2}$	0.5	0.5
pH	7.4	7.2-7.4

Characterization by X-ray diffraction

XRD is carried out for structural identification of the pure HA and HA-HT. X-ray diffraction patterns are recorded with a Bruker AXS Germany make X-ray diffractometer, having CuK (1.5405 Å) incident radiation. The XRD peaks are recorded in 2 theta range of 20–80◦.

Fourier Transform Infrared Spectroscopy

Bomen MB 100 FTIR spectrophotometer is used for determination of functional groups by scanning the HAp sample in the range of 400–4000 cm^{-1} with a resolution of 4 cm^{-1}.

SEM/EDS analysis

The surface morphology and microstructure of the samples before and after incubation is visualized by means of Scanning Electron Microscopy (JSM/JEOL-6360). All the samples are coated with thin film of gold (Au) to reduce charging of the sample. Simultaneously the elemental compositions of the samples are analyzed by using Energy Dispersive Spectroscopy (EDS). The experiment is performed at an accelerating voltage 20 kV and probe current 1 nA with counting rate 9755 cps and energy range 0–20 keV.

Inductive coupled plasma atomic emission spectroscopy

The concentrations of Ca, Si, ions in SBF after soaking were tested using inductive coupled plasma atomic emission spectroscopy (ICP-AES; Zaies 110394c)

X-ray fluorescence spectrometry

The elemental analysis of hydroxyapatite powder (raw material) was performed by X-ray fluorescence spectrometry (XRF, Bruker-S4 Pioneer, Germany).

To investigate the compressive strength of the produced sample the ASTM standard No. C0020-00R05 was utilized.

Based on that, if D is the diameter of the sample, the following equation is used:

$$CCS (kgf/cm^2) = F/\Pi D^2/4 \qquad (1)$$

Results and discussion

The apparent porosity and density of produced samples before TSS sintering are listed in Table 3.

Table 3. Apparent porosity and density of produced samples.

Sample	Apparent Porosity (%)	Density (gr/cm^3)
HA	30.9	2.12
HA5S	23.2	2.31
HA10S	18.3	2.44
HA15S	18.9	2.42

The values presented in this table suggest that with increasing the amount of HT up to 10% the apparent porosity is decreased to 18.3% so that a density of 2.44 gr/cm^3 obtained in this percentage of HT. It is also extracted from this table that the optimum value of density has been obtained in HA-10%HT nanocomposite and this percentage of HT could improve the density of HA up to 0.32. Figure 3 shows the results of compressive strength of the composite samples (before sintering). As can be seen in this figure, a maximum of 37.8 MPa has been obtained for CCS at about 10% HT which is consistent with the values presented in Table 3. The results of this section show that adding HT to HA can improve the mechanical properties of HA, significantly.

Fig. 4 shows the variation of intensity of diffracted X-rays as a function of value for the pure HAp (Fig. 4a), HA-15%HT (Fig. 4b), after TSS sintering. It is observable in Fig. 4 that a HA-15%HT nonocomposite without any additional phases has formed after high energy ball milling and subsequent TSS sintering. SEM images of the composite samples sintered with TSS process are shown in Fig. 5. As can be seen in Figs. 5a, b, c, with increasing amount of Hardystonite up to 10% reinforced in HA matrix, the congestion increases. It seems that the formation of Hardystonite silicate phases between the matrix particles led to the formation of glass bonds and hence increasing density.

According to Figure 5d, when the amount of HT reaches to 15%wt, the congestion starts to wane which is attributed to the overlapping of glass bonds and their subsequent failure.The bioactivity of ceramics has been defined as "the bond ability with host bone tissue" [14]. This includes enhancing the ability of apatite formation on the surface of samples in the SBF. This process can be analyzed by the dissolution curves. Dissolution curves that indicate the changes in calcium ions concentration and PH values versus immersion time in simulated body fluids are shown in Figure 6. As can be seen this

figure, in all percentages of HT (0, 5, 10 and 15), the PH value has been increased during first week of experiments which this is attributed to the three key factors:

1- Higher concentration of Ca ions in natural hydroxyapatite in comparison with non-natural one (Ca/P for natural and non-natural hydroxyapatite is 3.33 and 2.69, respectively. See EDX analysis), leads to instability of HA-HT nanocomposite and the entry of calcium ions into the SBF solution.

2- Replacement of the preliminary alkali ions with hydrogen.

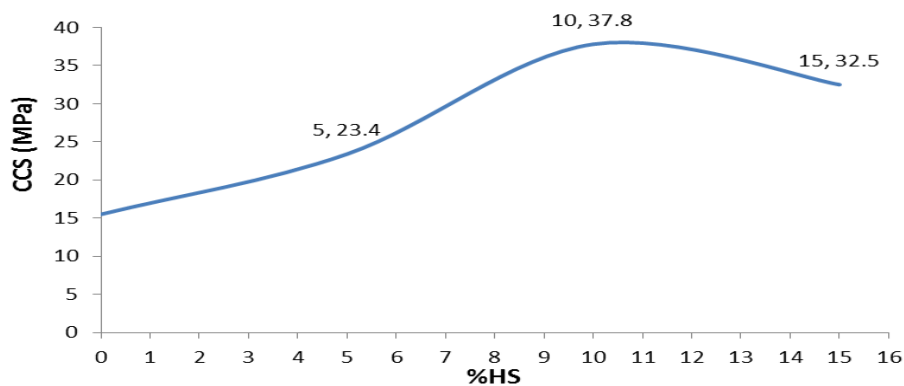3- Dissolution of the apatite matrix and releasing of the hydroxyl ions.

Figure 3. The results of compressive strength of the composite samples containing of different Hardystonite weight percent after sintering.
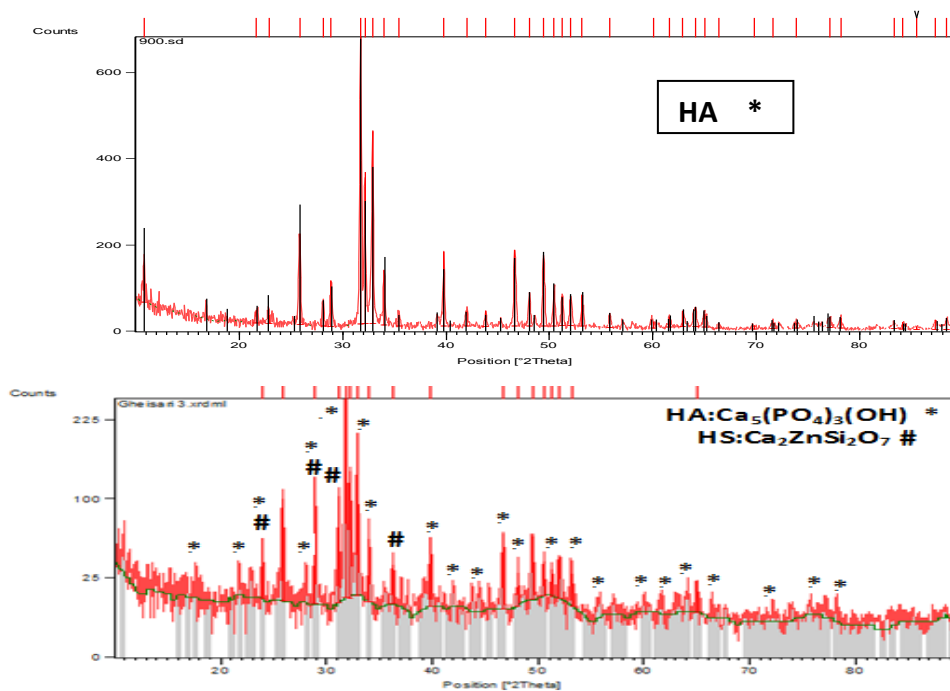

Figure 4. The variation of intensity of diffracted X-rays as a function of value for the pure HAp (a), HA-15%HT (b), after TSS sintering**.**

The dissolution curves suggest that the rate of change of pH values varies with increasing the percentage of HT in HA matrix. As can be seen in these curves, when the percentage of HT is 10, the pH has its lowest value at the first weekend (Figure 6.c), however when the amount of HT reaches 15%wt, the pH value decreases again (at the first weekend). This event originates from the more compressive strength of HA-HT nanocomposite resulted by increased HT up to 10%wt and hence less reacting with the SBF solution in the first week (see the Table 1, Figure 3 and Figure 5).

It is notable that the HA with 0%wt HT has highest value of pH (Figure 6a), because the concentration of Ca in HA - 0%wt HT is less than one in other HA-HT nanocomposite samples.It should be noted that when the calcium ions are released from the surface, many silanol (Si-OH) groups are formed on the surface. These Si-OH groups make the apatite nucleation heterogeneous. In the next stage, the solution is saturated from the Ca ions so that calcium ions tend to leave the solution. There are two places for their return. First, the surface of apatite nuclei and second the surface that the apatite has not formed on it. It is clear that, the Ca concentration in the surface of apatite nuclei is less than other surfaces so that the Ca ions (in the form of CaP ions) in the solution tend to move toward the apatite nuclei. This is a mechanism for growth of apatite layer in SBF solution. The movement of calcium ions into the surface of apatite nuclei leads to the pH decrease in the second week (Figure 6). The concentration of Ca ions at the second weekend in the SBF solution is dependent on the Si-OH nucleation sites. In other word, as these nucleation sites increase, the adsorption of calcium ions into these sites increases so that the concentration of Ca ions in the SBF solution are reduced (Figure 6a-d).
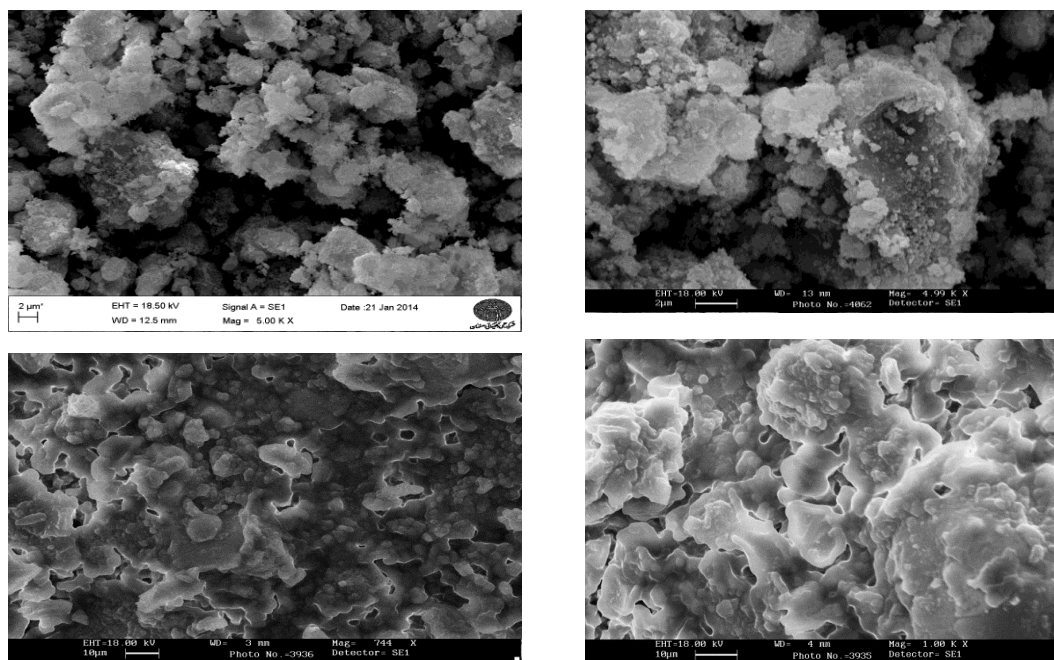

Figure 5. SEM images of the composite samples sintered with TSS process; a) 0%, b) 5%, c) 10% and d) 15% Hardystonite.
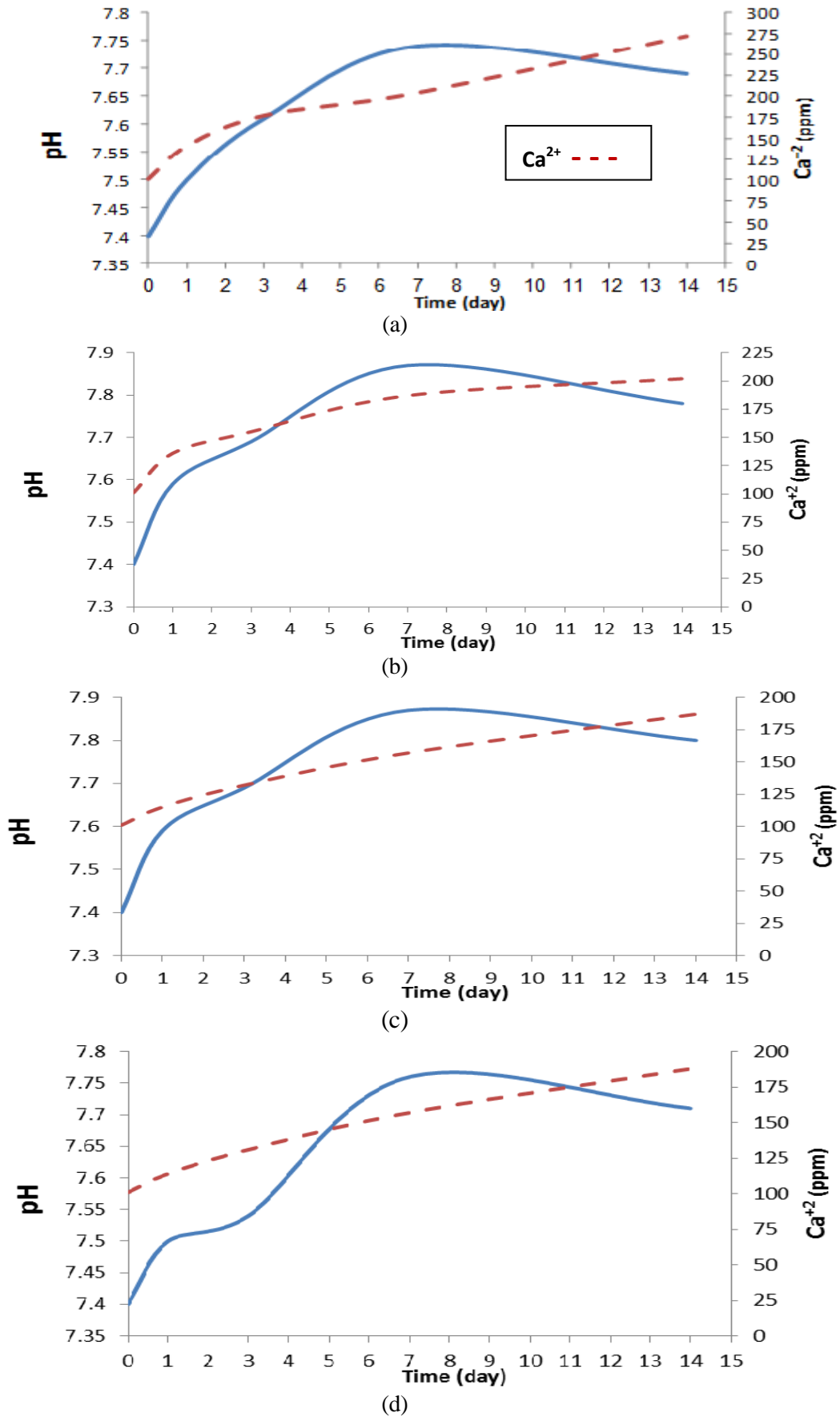
Figure 6. Dissolution curves indicating the changes in calcium ions concentration and pH values versus immersion time in simulated body fluids; a) HA-0%HT; b) HA-5%HT; c) HA-10%HT; d) HA-15%HT.

The above results are confirmed by SEM photographs and EDX analysis. SEM images of the samples after immersion in SBF solution for 14 days (second weekend) are shown in Figure 7. As can be seen in this figure, the apatite formation ability of HA-0%HT is very small compared to other samples of HA-HT nanocomposit (Figure 7a). As can be seen in Figure7 b, with increasing amount of Hardystonite to 5%wt, the apatite precipitations (Light porous areas) have been increased. As the amount of HT increases in the nanocomposite samples, the apatite formation on the surface of samples also increases (Figure 7c, d), which this is attributed to the more availability of nucleation sites for the Si-OH groups. This is confirmed by the EDX analysis which is discussed below.

The EDX analysis of samples with 10% and 15% HT (points A, B in Figure 7c, d) are shown in Figure 8. As can be seen in this figure, the surface that the apatite layer has not been formed on it (point B), has a higher Ca concentration than the surface of apatite layer (point A). This confirms what was said in this study about the growth of the apatite layer. On the other hand, the samples with higher amount of HT, have a more Si than the samples with a lower amount of HT. This is also confirms that with increasing the percentage of HT up to 15, the Si-OH nucleation sites also increases lead to ease of formation of apatite layers.
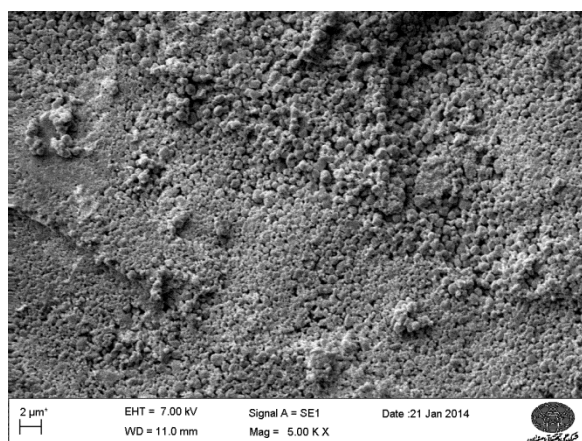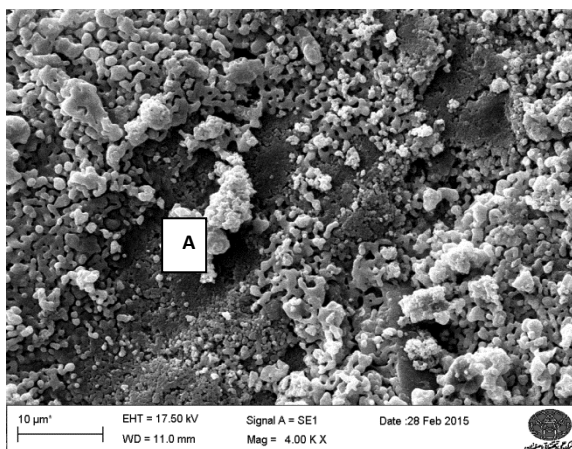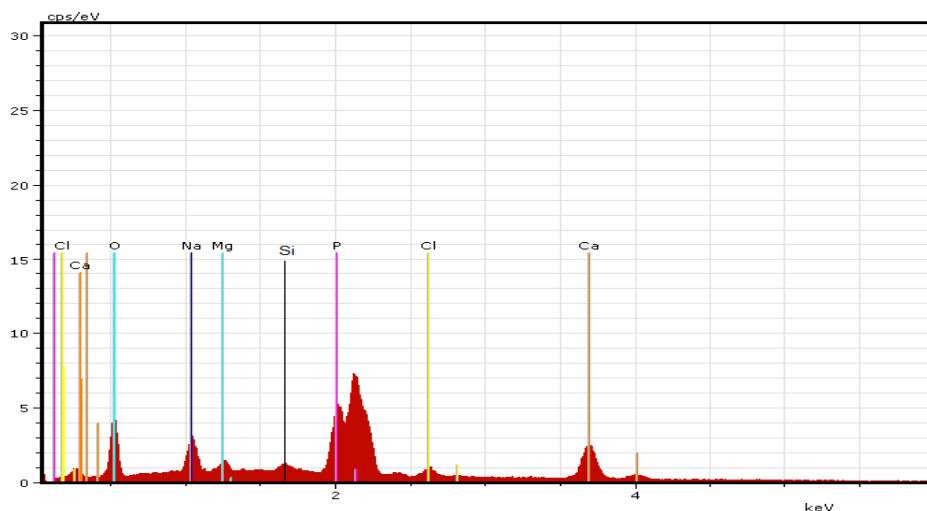

a
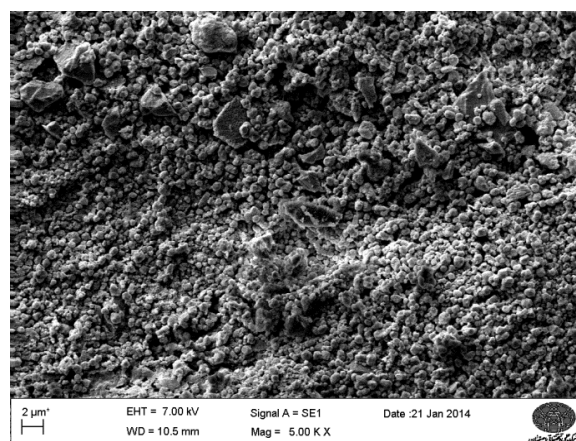
b
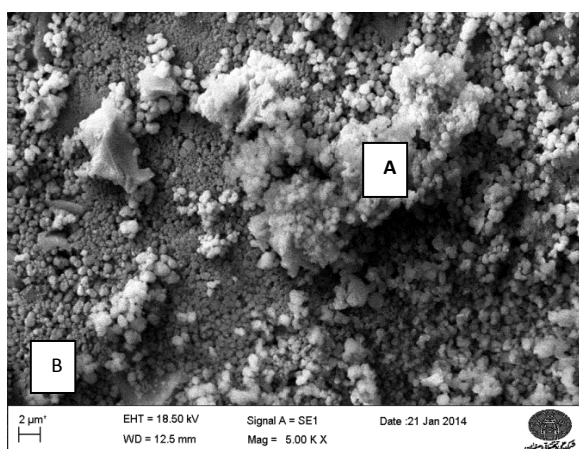
c

d

Figure 7. SEM images of the samples after immersion in SBF solution for 14 days ; a) HA-0 wt.%HT; b) HA-5wt.%HT; c) HA-10wt.%HT; d) HA-15wt.%HT.

Hydroxyapatite-hardystonite bio-nanocomposite

(a)

Element	series	wt.%	norm. wt.%
Oxygen	K-series	10.56687	19.79112
Sodium	K-series	2.588508	4.848121
Silicon	K-series	0.508765	1.000002
Magnesium	K-series	0.228531	0.364495
Phosphorus	K-series	10.48863	19.64458
Chlorine	K-series	1.238128	2.31894
Calcium	K-series	27.78132	52.03274
	Sum:	53.39199	100
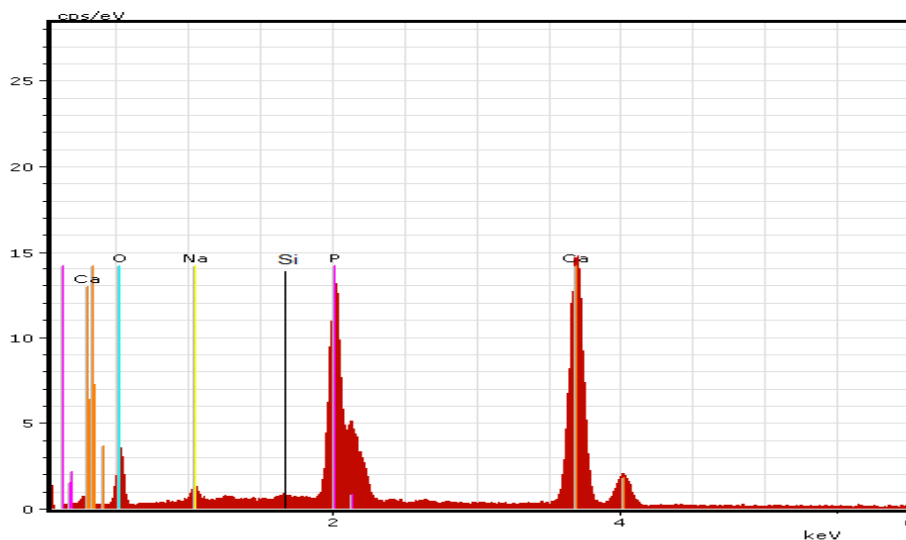
(b)

Element	Series	wt.%	norm. wt.%
Oxygen	K-series	22.46728	26.86663
Sodium	K-series	1.000002	1.001026
Silicon	K-series	0.390889	0.663241
Phosphorus	K-series	15.64122	18.70395
Calcium	K-series	44.12585	52.76618
	Sum:	83.62525	100

(c)
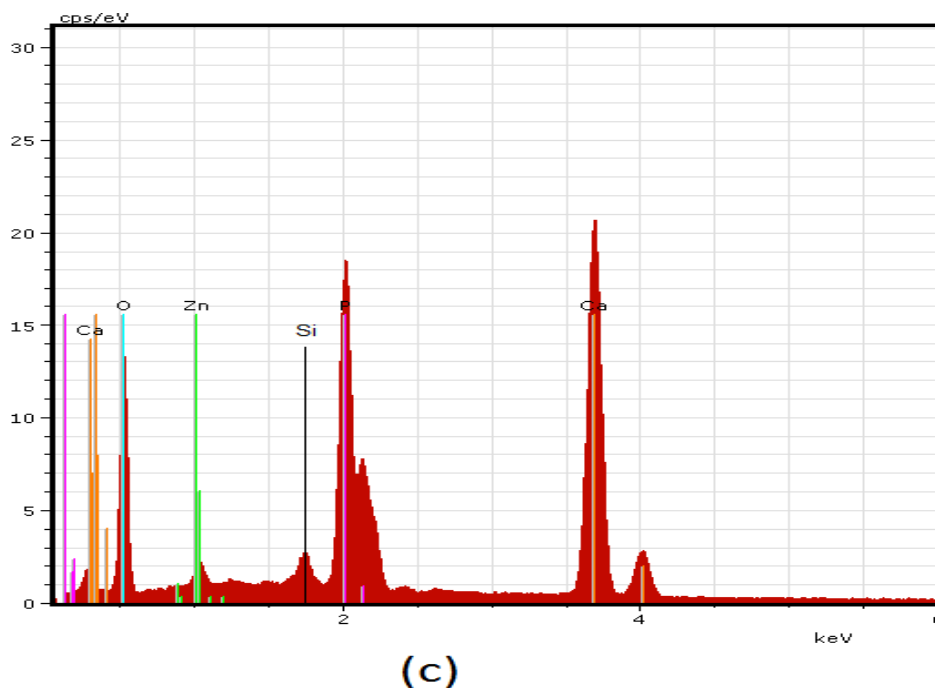
Element	Series	wt.%	norm. wt.%
Oxygen	K-series	43.08311	46.10041
Silicon	K-series	0.770121	0.824056
Phosphorus	K-series	10.61332	11.35661
Calcium	K-series	36.87211	39.45442
Zinc	K-series	2.116294	2.264507
	Sum:	93.45495	100

Figure 8. The EDS point analysis of samples with 10 wt. % (points A, B in Figure 7c) and 15 wt.% HT (points A, in Figure 7d)

Conclusions

The present study led to the following important conclusions. 1) The optimum value of density has been obtained in HA-10%HT nanocomposite samples so that this percentage of HT could improve the density of HA up to 0.32. 2) A maximum value of 37.8 MPa was obtained for the compressive strength of HA-10%wt HT nanocomposite sample. 3) It seems that the formation of Hardystonite silicate phases between the matrix particles led to the formation of glass bonds and hence increasing density of samples. When the amount of HT reaches to 15%wt, the density starts to wane. This is attributed to the overlapping of glass bonds and their subsequent failure. 4) In all percentages of HT (0, 5, 10 and 15), the pH value of samples has been increased during the first week of experiments. 5) Higher concentration of Ca ions in the natural hydroxyapatite in comparison with non-natural one, led to the movement of calcium ions into the solution and increasing the pH. 6) When the percentage of HT was 10, the pH had its lowest value at the first weekend however when the amount of HT reached 15%wt, the pH value increased again (at the first weekend). This event originates from the more compressive strength of HA-HT nanocomposite resulted by increased HT up to 10%wt and hence less reacting with the SBF solution in the first week. 7) As the Si-OH nucleation sites increase, the adsorption of calcium ions into these sites increases so that the concentration of Ca ions in the SBF solution is reduced. 8) The samples with higher amount of HT, have a more Si than the samples with a lower amount of HT. This is also confirms that

with increasing the percentage of HT up to 15, the Si-OH nucleation sites also increases lead to ease of formation of apatite layers.

Acknowledgments

References

1. Jaiswal AK, Chhabra H, Kadam SS, Londhe K, Soni VP, Bellare JR. Hardystonite improves biocompatibility and strength of electrospun polycaprolactone nanofibers over hydroxyapatite: A comparative study. Mater Sci Eng C Mater Biol Appl. 2013; 33: 2926–2936.

2. Zreiqat H, Ramaswamy Y, Wu C, Paschalidis A, Lu Z, James B, Birke O, McDonald M, Little D, Dunstan CR. The incorporation of strontium and zinc into a calcium–silicon ceramic for bone tissue engineering. Biomaterials. 2010; 31: 3175–3184.

3. Ramaswamy Y, Wu C, Zhou H, Zreiqat H. Biological response of human bone cells to zinc-modified Ca–Si-based ceramics. Acta Biomater. 2008; 4: 1487–1497.

4. Zhang W1, Wang G, Liu Y, Zhao X, Zou D, Zhu C, Jin Y, Huang Q, Sun J, Liu X, Jiang X, Zreiqat H. The synergistic effect of hierarchical micro/nano-topography and bioactive ions for enhanced osseointegration. Biomaterials. 2013; 34: 3184e3195.

5. Wu C. Methods of improving mechanical and biomedical properties of Ca-Si-based ceramics and scaffolds. Expert Rev Med Devic. 2009; 6: 237 – 241.

6. Ramaswamy Y, Wu CT, Zhou H, Zreiqat H. Biological response of human bone cells to zinc-modified Ca-Si-based ceramics. Acta Biomater. 2008; 4: 1487e97.

7. Wu C, Chang J, Wang J, Ni S, Zhai W. Preparation and characteristics of a calcium magnesium silicate (bredigite) bioactive ceramic. Biomaterials 2005; 26: 2925e31.

8. Mohammadi H, Hafezi M, Nezafati N, Heasarki S, Nadernezhad A, Ghazanfari S MH, pantafar M, Bioinorganics in Bioactive Calcium Silicate Ceramics for Bone Tissue Repair: Bioactivity and Biological Properties. J Ceram Sci Tech. 2014; 5(1): 1-12.

9. Chengtie Wu and yin Xiao, evaluation of the In VitroBioactivity of Bioceramics, Bone and Tissue Regeneration Insights. 2009; 2: 25–29.

10. Ji-Ho Park, Doug-Youn Lee, Keun-Taek Oh, Yong-Keun Lee, Kwang-Mahn Kim, Kyoung-Nam Kim. Bioactivity of calcium phosphate coatings prepared by electrodeposition in a modified simulated body fluid, Mater Lett. 206; 60: 2573–2577.

11. W. L. Tham, W. S. Chow, Z. A. Mohd Ishak, Simulated body fluid and water absorption effects on poly(methyl methacrylate)/hydroxyapatite denture base composites. eXPRESS Polymer Letters. 2010; 4(9): 517–528.

12. Pradnya N. Chavan, Manjushri M. Bahir, Ravindra U. Mene, Megha P. Mahabole, Rajendra S. Khairnar. Study of nanobiomaterial hydroxyapatite in simulated body fluid:Formation and growth of apatite, Materials Science and Engineering B. 2010; 168: 224–230.

13. Kokubo T, Takadama H. How useful is SBF in predicting in vivo bone bioactivity. Biomaterials. 2006; 27(15): 2907–15

14. Hench LL. Bioceramics: from concept to clinic. J Am Ceram Soc. 1991; 74: 1487–510.